



# Linking core-collapse supernova explosions to supernova remnants through 3D MHD modeling

S. Orlando<sup>1</sup>, A. Wongwathanarat<sup>2</sup>, H.-T. Janka<sup>2</sup>, M. Miceli<sup>1,3</sup>, M. Ono<sup>4</sup>, S. Nagataki<sup>4</sup>,  
F. Bocchino<sup>1</sup>, and G. Peres<sup>1,3</sup>

<sup>1</sup> INAF – Osservatorio Astronomico di Palermo, Piazza del Parlamento 1, Palermo, Italy  
e-mail: [salvatore.orlando@inaf.it](mailto:salvatore.orlando@inaf.it)

<sup>2</sup> Max-Planck-Institut für Astrophysik, Karl-Schwarzschild-Str. 1, Garching, Germany

<sup>3</sup> Dip. di Fisica e Chimica, Università di Palermo, Piazza del Parlamento 1, Palermo, Italy

<sup>4</sup> ABBL, RIKEN Cluster for Pioneering Research, 2-1 Hirosawa, Wako, Saitama, Japan

<sup>5</sup> RIKEN, iTHEMS Program, 2-1 Hirosawa, Wako, Saitama, Japan

**Abstract.** The structure and morphology of supernova remnants (SNRs) reflect the properties of the parent supernovae (SNe) and the characteristics of the inhomogeneous environments through which the remnants expand. Linking the morphology of SNRs to anisotropies developed in their parent SNe can be essential to obtain key information on many aspects of the explosion processes associated with SNe. Nowadays, our capability to study the SN-SNR connection has been largely improved thanks to multi-dimensional models describing the long-term evolution from the SN to the SNR as well as to observational data of growing quality and quantity across the electromagnetic spectrum which allow to constrain the models. Here we used the numerical resources obtained in the framework of the “Accordo Quadro INAF-CINECA (2017)” together with a CINECA ISCRA Award N.HP10BARP6Y to describe the full evolution of a SNR from the core-collapse to the full-fledged SNR at the age of 2000 years. Our simulations were compared with observations of SNR Cassiopeia A (Cas A) at the age of  $\sim 350$  years. Thanks to these simulations we were able to link the physical, chemical and morphological properties of a SNR to the physical processes governing the complex phases of the SN explosion.

**Key words.** hydrodynamics – instabilities – shock waves – ISM: supernova remnants – X-rays: ISM – supernovae: individual (Cassiopeia A)

## 1. Introduction

Supernova remnants (SNRs), the outcome of supernova (SN) explosions, are diffuse extended sources with a complex morphology and a highly non-uniform distribution of ejecta. General consensus is that such morphology reflects, on one hand, the physical and chemical properties of the parent SN and, on

the other hand, the properties of the progenitor stars and the early interaction of the SN blast wave with the circumstellar medium (CSM). Thus investigating the link between the morphological properties of a SNR and the complex phases in the SN explosion may help:

1) to trace back the characteristics of the asymmetries that may have occurred during

- the SN explosion, providing a physical insight into the processes governing the SN engines;
- 2) to identify the imprint of the progenitor stars, thereby obtaining information on the final stages of the stellar evolution.

However, studying the connection between SNRs and their parent SNe is an extremely challenging task which requires a multi-physics, multi-scale, multi-dimensional approach, due to the rich physics involved during the SN explosion and the subsequent expansion of the remnant, the very different time and space scales involved in these phases of evolution, and the inherent 3D nature of the anisotropies developing during the whole evolution. To overcome all these difficulties, we adopted an approach based on the coupling between core-collapse SN models and SNR models (e.g. Orlando et al. 2015, 2016; Wongwathanarat et al. 2017; Ferrand et al. 2019; Ono et al. 2020; Orlando et al. 2020; Tutone et al. 2020; Gabler et al. 2020).

Here we studied the ejecta dynamics of the SNR Cas A from the core-collapse SN explosion to their expansion in the SNR by linking, for the first time, modeling attempts that have been carried out independently so far, either constrained to the early phase of the SN up to days only (Wongwathanarat et al. 2017), or starting the long-time remnant evolution with artificial initial conditions (Orlando et al. 2016). The simulations covered 2000 years of evolution, thus going beyond the age of Cas A ( $\approx 350$  years). The aim was to investigate how the final remnant morphology reflects the characteristics of the SN explosion and, in particular, the asymmetries that develop in the immediate aftermath of the core-collapse

## 2. The model

We focused on a SN model which reproduces post-explosion anisotropies, one day after the SN event, which are compatible with the structure of Cas A (Wongwathanarat et al. 2017): three pronounced nickel-rich fingers that may correspond to the extended iron-rich regions observed in Cas A. These simulations provided the initial conditions for our 3D

SNR simulations soon after the shock breakout. The plasma and magnetic field evolution were modeled numerically by solving the time-dependent MHD equations, including the deviations from electron-proton temperature-equilibration, and the deviations from equilibrium of ionization of the most abundant ions, in a 3D Cartesian coordinate system (see Orlando et al. 2021 for the detail of the implementation). These effects are necessary to describe appropriately the evolution of the remnant and to synthesize accurately the thermal X-ray emission from model results. We also included the effects of heating due to radioactive decay of  $^{56}\text{Ni}$  and  $^{56}\text{Co}$ .

The calculations were performed using the PLUTO code (Mignone et al. 2007) a well tested modular Godunov-type code intended mainly for astrophysical applications and high Mach number flows in multiple spatial dimensions. The initial density, pressure, and velocity structure of ejecta as well as the isotopic composition of the ejecta were derived from the adopted SN simulation (Wongwathanarat et al. 2017). Then the 3D SNR simulations describe the interaction of the remnant with the wind of the progenitor star. The wind was assumed to be spherically symmetric with gas density proportional to  $r^{-2}$  (where  $r$  is the radial distance from the progenitor). In order to compare the simulations with Cas A, the wind density at  $r = 2.5$  pc was constrained by X-ray observations of the shocked wind in this remnant (Lee et al. 2014).

We performed multi-species simulations to follow the evolution of the isotopic composition of ejecta and the matter mixing and to link the chemical distribution of ejecta in the remnant to anisotropies developing in the early phases of SN evolution. A major challenge in modeling the explosion and subsequent evolution of the remnant was the very small scale of the system (the initial blast wave radius is  $\approx 10^{14}$  cm) in the immediate aftermath of the SN explosion ( $\approx 1$  day after the SN event) in comparison with the size of the rapidly expanding blast wave (a final size of  $\approx 8$  pc at the age of 2000 years). To capture this range of scales we adopted a strategy similar to that used by Orlando et al. (2019).

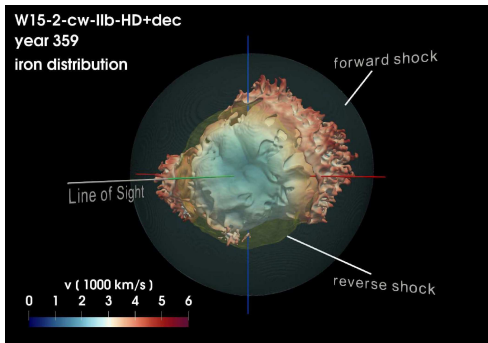


**Fig. 1.** Isosurface of the distribution of iron at the age of Cas A for one of our simulations (see Orlando et al. 2021). The opaque isosurface correspond to a value of Fe density which is at 5% of the peak density; the colors give the radial velocity in units of  $1000 \text{ km s}^{-1}$  on the isosurface. The semi-transparent quasi-spherical surfaces indicate the forward (green) and reverse (yellow) shocks. The Earth vantage point lies on the negative  $y$ -axis. A navigable 3D graphic of this distribution is available at <https://skfb.ly/6TKRK>.

### 3. Results

The model and the results of our analysis are presented in detail in Orlando et al. (2021); here we summarize our main findings.

We explored the effects of energy deposition from radioactive decay and the effects of an ambient magnetic field on the evolution of the remnant, by performing three long-term simulations with the above effects switched either on or off. In all the cases, our simulations predict radii of the forward and reverse shocks and ejecta velocities at the age of  $\approx 350$  years consistent with those observed in Cas A. We found that the fundamental chemical, physical, and geometric properties observed in Cas A can naturally be explained in terms of the physical processes associated with the asymmetric SN explosion and to subsequent interaction of the initial asymmetries with the reverse shock of the SNR.

The ejecta distribution soon after the breakout of the shock wave at the stellar surface is characterized by large-scale plumes of ejecta rich in  $^{56}\text{Ni}$  and  $^{44}\text{Ti}$  (Wongwathanarat et al. 2017). One year later, the  $^{56}\text{Ni}$  decayed in

$^{56}\text{Co}$  and the latter in stable  $^{56}\text{Fe}$ . The high-entropy plumes of Fe- and Ti-rich ejecta cross the reverse shock at the age of  $\approx 30$  years. This interaction triggers the development of hydrodynamic (HD) instabilities which gradually fragment the plumes into numerous small-scale fingers. At the age of Cas A, the shocked portion of these plumes lead to the formation of extended regions of shock-heated Fe similar to those observed in Cas A. The fine-scale structure of the plumes and the HD instabilities triggered by the reverse shock lead to the formation of a filamentary pattern of shocked ejecta with ring-like and crown-like features (see Fig. 1) which resembles that observed in Cas A remarkably well (e.g. Milisavljevic & Fesen 2013). The initial large-scale plumes are also responsible for the spatial inversion of the ejecta layers with Si-rich ejecta being physically interior to Fe-rich ejecta. The inversion is evident only in regions where the fast plumes of Fe-rich ejecta interact with the reverse shock; elsewhere, the original chemical stratification is roughly preserved.

The unshocked ejecta of the modeled remnant show voids and cavities similar to those observed (e.g. Milisavljevic & Fesen 2015; see Fig. 2). They originate from the expansion of Fe-rich plumes and their inflation due to the decay of radioactive species. We found that the largest cavities are physically connected with the large-scale Si-rich rings of shocked ejecta which encircle the Fe-rich regions. The initial large-scale asymmetry is also responsible for the metal-rich ejecta being arranged in a “thick-disk” geometry. The disk is tilted with respect to the plane of the sky as inferred from observations of Cas A. The distributions of  $^{44}\text{Ti}$  and  $^{56}\text{Fe}$  are mostly concentrated in the northern hemisphere, pointing opposite to the kick velocity of the neutron star. These distributions and their abundance ratio are both compatible with those inferred from high-energy observations of Chandra and NuSTAR (Grefenstette et al. 2014, 2017).

Finally, the simulations showed that, after 2000 years of evolution, most of the metal-rich ejecta were shocked and subject to strong mixing by the HD instabilities. However, the spatial distributions of iron-group elements,

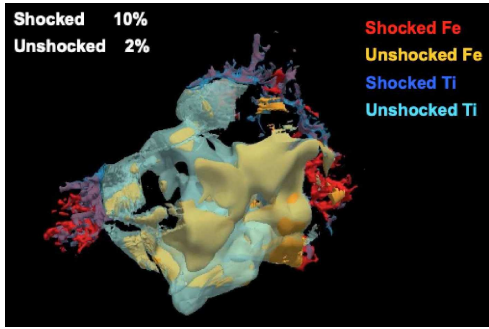


**Fig. 2.** Isosurfaces of the distribution of iron and titanium at the age of Cas A for one of our simulations (see Orlando et al. 2021). The irregular isosurfaces correspond to a value of Fe and Ti density at 10% (shocked) or 2% (unshocked) of the maximum density; the colors indicate either shocked or unshocked Fe and Ti as reported in the upper right corner.

the decay product of Ti ( $^{44}\text{Ca}$ ) and Si still keep memory of the original SN asymmetry. Furthermore, cavities and voids in the unshocked ejecta are still evident even though more diluted than in previous epochs. We concluded that the fingerprints of the SN can still be found  $\approx 2000$  years after the explosion.

#### 4. Conclusions

Our study has shown that the structures observed in the inter-shock region of a core-collapse SNR are the natural consequence of the interaction of the reverse shock with the post-explosion large-scale asymmetries of the SN. In particular, the main features observed in the morphology of Cas A (Fe-rich regions, ring- and crown-like features, inversion of ejecta layers, etc.) develop as a consequence of the fast growth of HD instabilities in the reverse-shock heated plumes of ejecta developed after the SN explosion. All these features encode the fingerprints of a neutrino-driven SN explosion. Our simulations, therefore, provided more conclusive information whether the paradigm of the neutrino-driven explosion mechanism is able to explain the chemical and morphological asymmetries observed in great detail in Cas A, a young remnant of a stripped-envelope (type IIb) SN.

*Acknowledgements.* The PLUTO code is developed at the Turin Astronomical Observatory (Italy) in collaboration with the Department of General Physics of Turin University (Italy) and the SCAI Department of CINECA (Italy). We acknowledge the “Accordo Quadro MoU per lo svolgimento di attività congiunta di ricerca Nuove frontiere in Astrofisica: HPC e Data Exploration di nuova generazione” and CINECA ISCRA Award N.HP10BARP6Y for the availability of high performance computing resources and support at the infrastructure Marconi based in Italy at CINECA. At Garching, funding through ERC-AdG no. 341157-COCO2CASA and DFG grants SFB-1258 and Cluster of Excellence ORIGINS (EXC-2094)390783311 is acknowledged. Computer resources have been provided by MPCDF.

#### References

- Ferrand, G., Warren, D. C., Ono, M., et al. 2019, *ApJ*, 877, 136
- Gabler, M., Wongwathanarat, A., & Janka, H.-T. 2020, arXiv e-prints, arXiv:2008.01763
- Grefenstette, B. W., Fryer, C. L., Harrison, F. A., et al. 2017, *ApJ*, 834, 19
- Grefenstette, B. W., Harrison, F. A., Boggs, S. E., et al. 2014, *Nature*, 506, 339
- Lee, J.-J., et al. 2014, *ApJ*, 789, 7
- Mignone, A., Bodo, G., Massaglia, S., et al. 2007, *ApJS*, 170, 228
- Milisavljevic, D. & Fesen, R. A. 2013, *ApJ*, 772, 134
- Milisavljevic, D. & Fesen, R. A. 2015, *Science*, 347, 526
- Ono, M., Nagataki, S., Ferrand, G., et al. 2020, *ApJ*, 888, 111
- Orlando, S., Miceli, M., Petruk, O., et al. 2019, *A&A*, 622, A73
- Orlando, S., et al. 2015, *ApJ*, 810, 168
- Orlando, S., et al. 2016, *ApJ*, 822, 22
- Orlando, S., Ono, M., Nagataki, S., et al. 2020, *A&A*, 636, A22
- Orlando, S., Wongwathanarat, A., Janka, H. T., et al. 2021, *A&A*, 645, A66
- Tutone, A., Orlando, S., Miceli, M., et al. 2020, arXiv e-prints, arXiv:2009.01157
- Wongwathanarat, A., et al. 2017, *ApJ*, 842, 13